Item DR1: LiDAR scanning and Luminescence dating at the Raham Chronosequence.

The Raham chronosequence (Fig. DR1) was previously studied by Crouvi et al. (2006), who identified and mapped five distinct late Quaternary terraces. The two older terraces mapped at Raham, Ra-Q1 and Ra-Q2, were scanned with ground-based LiDAR following the procedures outlined in the main text.

Figure DR1. Top – Google Earth image of the studied chronosequences north of the Gulf of Aqaba. Bottom – the late Quaternary Raham terraces examined in this study and point-cloud rendering of their LiDAR scans.

Luminescence sampling and analytical procedures:

In the present study, we determined a luminescence abandonment age for the older terraces mapped by Crouvi et al. (2006). Ra-Q1 (56 ± 10 ka) and Ra-Q2 (24 ± 3 ka). Sample collection was based on the mapping results of Crouvi et al. (2006) (Fig. DR2). Ra-Q2 was sampled within an excavated trench following a detailed examination of the soil profile. The three samples for Ra-Q2 were extracted from 30 cm depth. Ra-Q1 was sampled within a local drainage ditch following a detailed examination of the soil profile. Sample depth was 40 cm below the pavement. Gamma and cosmic doses were measured in the field using a portable gamma scintillator.

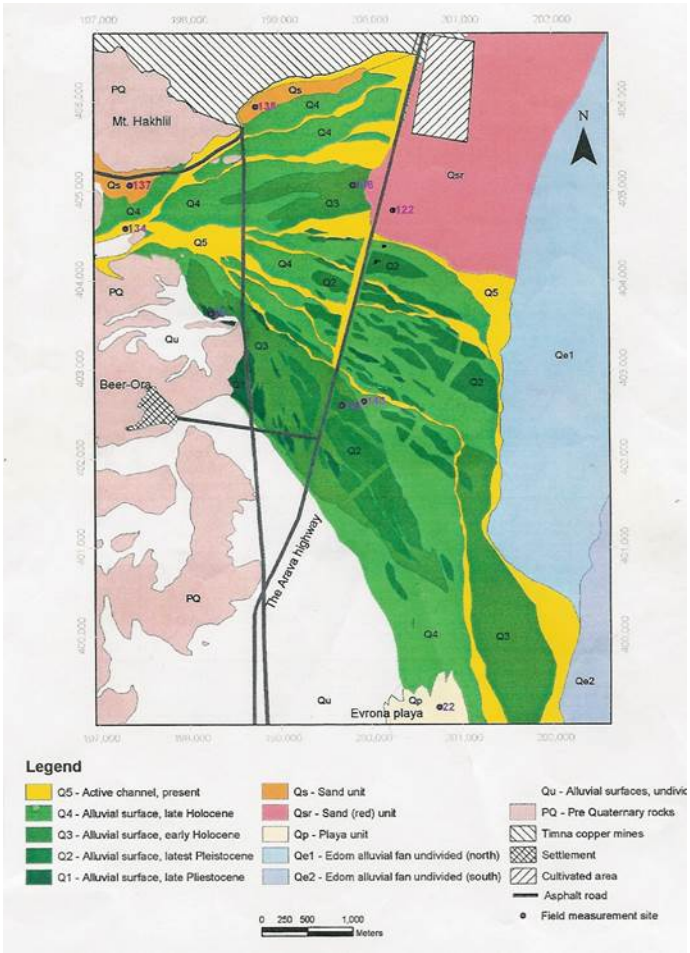

Figure DR2. Geomorphic map of the terraces comprising the Raham Chronosequence. From Crouvi et al. (2006)

For all processed samples, 88-125 μm Quartz fraction was extracted using routine laboratory procedures (Porat et al., 2010; 2012). De was measured on 8-mm aliquots using the optically stimulated luminescence (OSL) signal and the single aliquot regenerative (SAR) dose protocol. Alpha and beta dose rates were calculated from the concentrations of the radioactive elements U, Th and K, measured by ICP-MS. Gamma and cosmic doses were measured in the field using a portable gamma scintillator. Water contents were estimated at 1±0.5 %. Recycling ratios are mostly between 0.95 and 1.05 (Table S2).

Table DR1: Luminescence measurements for Raham terraces Q1 and Q2.

Surface/ Sample	Depth (m)	K (%)	U (ppm)	Th (ppm)	ext. α (μGy/a)	ext. β (μGy/a)	Ext. γ (μGy/a)	Total dose (μGy/a)	No. of discs	De (Gy)	**Age (ka)**
Ra-Q2											
RT1-1	0.3	0.33	1.07	0.94	4	393	419	815±47	11/12	18.9±4.0	23±5
RT1-8	0.3	0.47	1.14	1.45	4	512	513	1029±56	9/10	22.4±4.2	22±4
RT1-19	0.3	0.35	1.17	1.11	4	424	496	924±54	9/12	24.6±5.9	27±7
										Average:	**24±3**
Ra-Q1											
BOR-4	0.4	0.45	1.7	1.6	5	560	540	1115±59	13/13	62.3±11.3	**56±10**

Item DR2: Definition of slope-moderation point.

A linear fit was constrained for all the PSD curves in Figure 2A at $10^{-1.35} < \lambda < 10^{-0.7}$ m. The moderation point (λ_m) was defined as the point at which the PSD curve falls below and deviates by more than 3σ of the residuals between observed PSD and the linear fit (Fig. DR3).

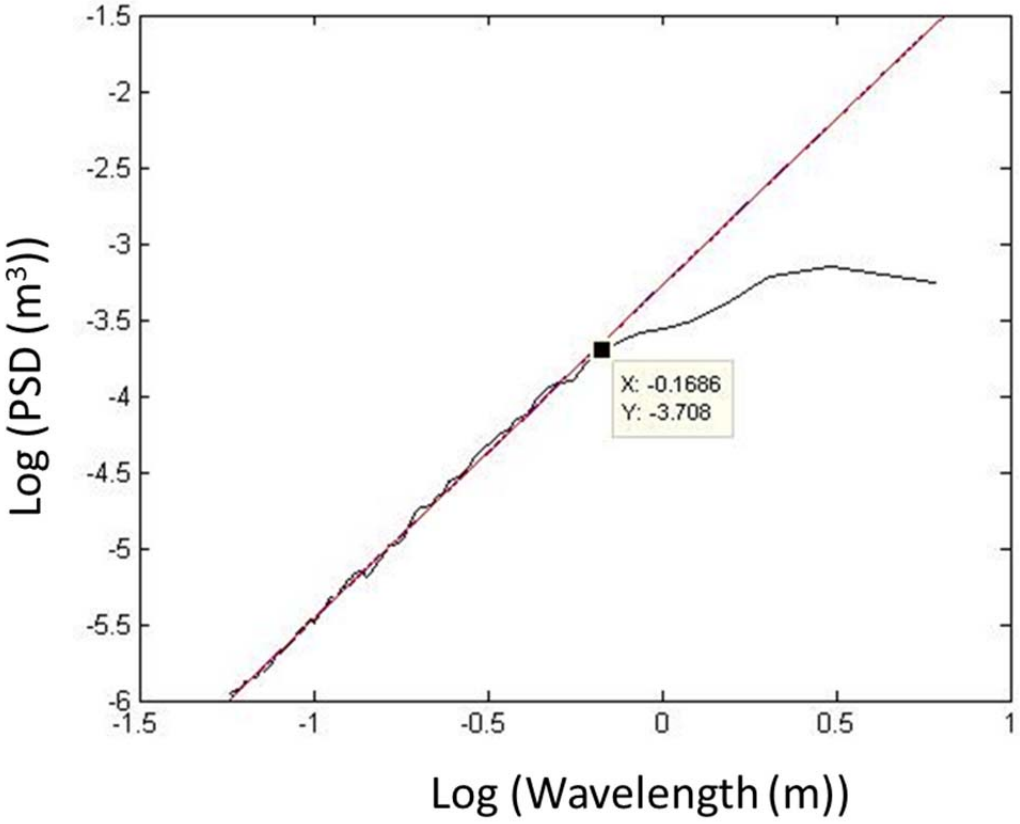

Figure DR3. Example for definition of the PSD slope moderation point for one of the Shehoret 14 ka curve in the log-log plot in Fig. 2A. Values on both axes are the powers of the logarithm presentation of PSD and Wavelength in Fig. 2A.

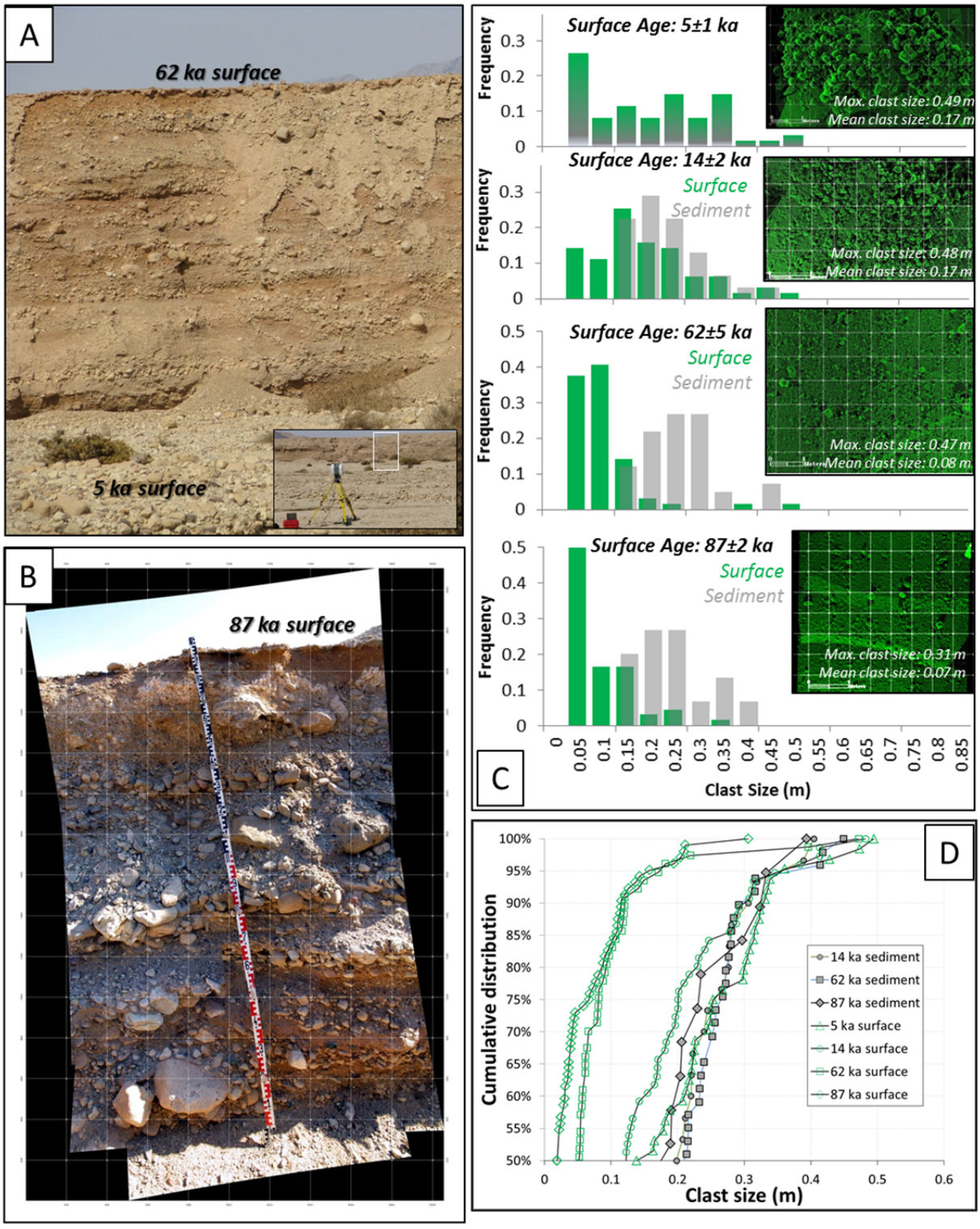

Figure DR4. Size-frequency distribution of rocks within the un-weathered alluvial sediments and on the surfaces of the Shehoret terraces. A: Cut-bank exposure (~5-m-high) of the 62 ka terrace C-horizon. In the foreground - 5 ka surface. White box in inset marks the location of this cut-bank exposure. B: Exposed C-horizon for the 87 ka terrace within an excavated trench (Amit et al., 1996). C-Horizon

exposures (14 ka not shown) reveal abundant decimeter-size boulders similar to those of the 5 ka surface within the un-weathered sediments of the older terraces and suggest similar depositional environments. C: Histograms describing the size-frequency distribution of cobbles-boulders within the un-weathered terrace sediments (grey bars) compared to rock distributions at the surfaces of the same terraces (green bars). The maximum and mean rock size for surface rocks are shown on the LiDAR scans presented on the right. The histograms demonstrate the non-normal distribution of rock sizes on some of the surfaces and the questionable use of 'standard' statistical measures such as the 'mean'. D. Cumulative size-frequency distribution of cobbles-boulders within the un-weathered terrace sediments (solid grey symbols) compared to rock distributions at the surfaces of the same terraces (open green symbols). The histograms (B) and size-frequency distribution curves (C) demonstrate: 1) Common initial pre-weathering depositional cobble-boulder distributions for all the Shehoret terraces that are similar to that of the minimally weathered 5 ka surface; 2) Time-progressive rock-size reduction (diminution) on these terraces is associated with pronounced changes in the size-frequency distribution; , and 2) 'Conventional' statistical parameters such as the maximum clast size and/or the mean do not correlate with surface age as previously shown for alluvial chronosequences elsewhere (McFadden et al.,1989; Frankel and Dolan, 2007).

Figure DR5. A typical Av horizon of several cm on the Shehoret Qa1b (~62 ka) terrace. Desert pavement rocks characteristically 'float' on top of the clast-free Av horizon.

TABLE DR2. SOIL CHARACTERISTICS FOR THE SHEHORET TERRACES

Terrace	Age (ka)	Horizon	Depth (cm)	Gravel (%)	Shattered gravel (%)	Lower Boundary	Gypsum (%)	EC (S/m)	Cations (meq/100 gr soil)			Sand (%)	Silt (%)	Clay (%)
									Ca	Mg	Na			
Sh-Qa4	4.6±0.7^{+}	Av	0-0.5	10	0	c	2.70	3.8	33.0	5.4	38.0	58.0	33.2	8.8
		Bw	0.5-1.5	70	0	a	3.30	5.0	30.0	6.8	57.0	36.5	41.7	21.8
		C1y	1.5-20	70	15	g	7.50	8.5	73.5	10.0	90.0	90.3	7.4	2.3
		C2	20-40	80	0	g	8.30	8.6	77.0	11.4	85.0	93.2	4.2	2.6
Sh-Qa3	14±2^{+}	A1	0-3.0	20	0	c	3.90	5.7	35.0	6.4	75.0	74.7	19.7	5.5
		A2	3-6	50	0	a	5.10	10.6	49.0	9.6	169.5	68.0	23.2	8.8
		Bw	6-8	20	0	c	7.80	16.1	88.0	14.6	265.0	63.5	24.8	11.8
		C1zy	8-28	60	60	g	8.20	12.6	90.0	15.6	169.0	85.4	10.0	4.6
		C2z	28-50	70	0	g	8.40	13.2	81.0	16.0	188.0	88.7	11.1	0.2
Sh-Qa1$_b$	62±5^{+}	Bg.f	0-5.0	2	0	c	1.6	2.8	9.5	3.3	23.5	49.3	38.7	12.0
		Cy	5.0-23	10	50	c	28.5	0.9	299.4	1.4	21.8	71.0	28.7	0.4
		Cy,z	23-41	45	10	g	8.7	1.5	63.6	2.5	8.2	60.7	38.8	0.5
		Cz	41-70	60	0	c	6.0	1.9	45.2	2.7	13.6	74.7	21.6	3.7
		Cz	70-85	60	0	g		22.8	33.4	1.6	742.2	88.3	9.1	2.6
		Cz	85-100	60	0	g		16.0	15.2	4.6	262.2	88.0	10.0	2.0
Sh-Qa1$_a$	87±2^{+}	Bg.f	0-10.0	5	0	c	1.0	1.7	5.0	1.6	9.8	55.3	32.7	12.0
		Cy	10.0-20	15	80	a	28.9	2.9	280.7	1.8	73.4	78.9	14.6	6.6
		Cy,z	20-40	25	10	g	14.8	2.1	89.7	2.0	13.6	56.4	40.2	3.4
		C	40-60	50	1	g	6.9	3.1	49.9	3.9	36.5	87.1	11.0	1.9
		Cz	60-75	60	0	a		22.6	27.2	1.6	831.1	87.3	10.5	2.3
		Cz	75-85	60	0	g		21.1	155.9	2.8	587.2	81.7	18.2	0.2
		sediment	85-100	60	0	g	1.7	1.4	12.5	1.6	13.6	77.6	22.1	